All-Scale Hierarchically Structured p-Type PbSe Alloys with High Thermoelectric Performance Enabled by Improved Band Degeneracy

Gangjian Tan,[*,†] Shiqiang Hao,[‡] Songting Cai,[‡,§] Trevor P. Bailey,[⁄⁄] Zhongzhen Luo,[§] Ido Hadar,[§] Ctirad Uher,[⁄⁄] Vinayak P. Dravid,[‡] Christopher Wolverton,[‡] and Mercouri G. Kanatzidis[*,§]

[†]State Key Laboratory of Advanced Technology for Materials Synthesis and Processing, Wuhan University of Technology, Wuhan 430070, P. R. China
[‡]Department of Materials Science and Engineering and [§]Department of Chemistry, Northwestern University, Evanston, Illinois
60208, United States
[⁄⁄]Department of Physics, University of Michigan, Ann Arbor, Michigan 48109, United States

ABSTRACT:

We show an example of hierarchically designing electronic bands of PbSe toward excellent thermoelectric performance. We find that alloying 15 mol % PbTe into PbSe causes a negligible change in the light and heavy valence band energy offsets (ΔE_V) of PbSe around room temperature; however, with rising temperature it makes ΔE_V decrease at a significantly higher rate than in PbSe. In other words, the temperature-induced valence band convergence of PbSe is accelerated by alloying with PbTe. On this basis, applying 3 mol % Cd substitution on the Pb sites of PbSe0.85Te0.15 decreases ΔE_V and enhances the Seebeck coefficient at all temperatures. Excess Cd precipitates out as CdSe1−yTey, whose valence band aligns with that of the p-type Na-doped PbSe0.85Te0.15 matrix. This enables facile charge transport across the matrix/precipitate interfaces and retains the high carrier mobilities. Meanwhile, compared to PbSe the lattice thermal conductivity of PbSe0.85Te0.15 is significantly decreased to its amorphous limit of 0.5 W m−1 K−1. Consequently, a highest peak ZT of 1.7 at 900 K and a record high average ZT of ∼1 (400−900 K) for a PbSe-based system are achieved in the composition Pb0.95Na0.02Cd0.03Se0.85Te0.15, which are ∼70% and ∼50% higher than those of Pb0.98Na0.02Se control sample, respectively.

1. INTRODUCTION

Thermoelectric materials that can reversibly and directly convert waste heat to electricity are drawing increased attention as a possible means to increase overall energy efficiency.[1] Maximizing thermoelectric conversion efficiency requires the materials to have high figure of merit ZT = S2σT/κ = S2σT/(κlat + κcar), where S represents Seebeck coefficient, σ is electrical conductivity, T is absolute temperature, and κ is thermal conductivity contributed by both lattices (κlat) and carriers (κcar). In reality, both high peak ZT and large average ZT,

$$ZT_{\text{ave}} = \int_{T_C}^{T_H} \frac{ZT}{T_H - T_C}\,\mathrm{d}T$$

where T_C and T_H denote the cold and hot side temperatures, respectively, are desired to achieve the best device performance.[2]

Among the materials suitable for thermoelectric power generation applications, PbTe has been the most studied, and new developments including recent advances of nanostructuring[3−5] and band-structure modification[6−8] have shown exceptional ZT values in both n- and p-type compositions. In contrast, PbSe, a close analogue of PbTe, is much less studied (despite its lower cost and higher melting point) because of its inferior band structure.[9,10] For example, both PbSe and PbTe feature two valence bands, one primary light valence band (LVB) L and another lower-lying heavy valence band (HVB) Σ, which are separated by an energy offset of ΔEV (see inset of Figure 2a).[11,12] This ΔEV is important because when its value becomes small enough (e.g., < ∼0.2 eV) at a given temperature, both bands contribute to the thermoelectric transport and a significant enhancement in power factor can be realized. This is the key reason for the record high performance achieved in p-type PbTe systems. At 300 K, the value of ΔEV is only ∼0.15−0.20 eV for PbTe, and it further decreases with increasing temperature at a rate of ∼4 × 10−4 eV/K.[11,13] As a result, it is possible to achieve effective band convergence (ΔEV is reduced to a few kBT, where kB is Boltzmann constant) in PbTe at relatively low temperatures (<700 K).[6] Even better valence band convergence can be attained in PbTe by chemical alloying with certain isovalent elements (e.g., Mn,[14] Cd,[15] Mg,[16] Sr,[7] etc.). This happens by lowering the energy of the L band but not the Σ band. It also enlarges the band gap. When band convergence is also accompanied by the introduction of carriers, it results in multiband transport and significantly enhances S without obviously deteriorating σ.6 However, in comparison with PbTe, the ΔEV of PbSe is almost twice as large (∼0.3−0.35 eV) at 300 K, and it decreases with temperature at a much lower rate of ∼2.2 × 10−4 eV/K (half that of PbTe).[11,17] Therefore, it is quite challenging to realize the thermoelectric benefit through valence band convergence in PbSe until much higher temperatures are reached (>1000 K).[9]

Several studies have focused on converging the LVB and HVB of PbSe through chemical alloying, with an attempt to enhance the Seebeck coefficient. For instance, Zhao et al. reported that Cd substitution for Pb can reduce ΔE_V of PbSe.[18] However, Cd has <3 mol % solubility around room temperature and precipitates out as CdSe second phase whose valence band maximum (VBM) has a large energy mismatch with that of PbSe matrix. This limits the degree to which the two bands can be converged and also causes high hole carrier scattering at the matrix/precipitate interfaces and worsens σ. Later, Wang et al. used a long-period, high-temperature annealing method to capture ∼8 mol % SrSe dissolvable into PbSe.[17] Although ΔE_V is decreased to a large extent and the peak ZT is enhanced from 1.1 to 1.5 at 900 K, it is still not enough to converge the two valence bands of PbSe at sufficiently low temperatures comparable to PbTe. There are possibly two reasons: (i) as we mentioned earlier, ΔEV decreases too slowly with temperature; (ii) SrSe solubility is not high enough to enable strong band convergence. Very recently, Hodges et al. alloyed PbSe with HgSe and observed a similar reduction of ΔEV.[19] They claimed a peak ZT of 1.7 at a very high temperature of 970 K.

In this contribution, we hierarchically design the electronic bands of PbSe by alloying with 15 mol % PbTe and 3 mol % CdSe to achieve effective valence band convergence at temperatures as low as 700 K. PbTe and CdSe alloying play different but synergistic roles in reducing ΔEV of PbSe. Specifically, PbTe alloying itself does not directly converge the LVB and HVB of PbSe. However, at high temperatures it allows ΔEV to drop much faster because PbTe

has a stronger temperature dependence of ΔEV than PbSe, as discussed earlier. CdSe alloying, on the other hand, further decreases ΔEV at all temperatures by chemically converging the valence bands. Therefore, in the PbSe system we have integrated two separate valence band-modifying effects: (i) faster valence band convergence with rising temperature (by introducing some PbTe) and (ii) better valence band convergence than PbSe by alloying with Cd. Excess Cd precipitates out as CdSe1−yTey second phase, the VBM of which aligns well with that of PbSe0.85Te0.15 matrix in energy, allowing the charge carriers to be less scattered at the matrix/precipitate interfaces and maintaining high carrier mobilities. These nanoscale precipitates, together with PbTe alloying and Cd substitution (see the schematic crystal figuration shown in Figure 1a), produce all-scale hierarchical structuring in PbSe, lowering κlat values to its minimum limit. As a result, a peak ZT of 1.7 at 900 K is obtained in the sample Pb0.95Na0.02Cd0.03Se0.85Te0.15, which is the highest among all reported values on p-type PbSe at the same temperature. More importantly, ZTave, the key parameter in determining the device performance from 400 to 900 K, is ∼1, the highest achieved in a PbSe system. This research opens new avenues toward high thermoelectric performance in bulk materials and enables PbSe to be a competitive candidate for mid-to-high temperature thermoelectric power generation applications.

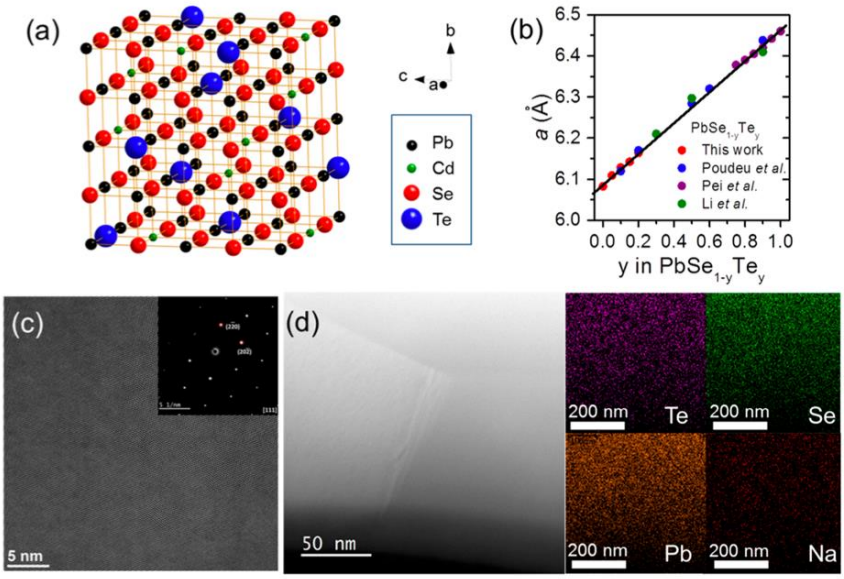

Figure 1. (a) Schematic crystal configuration of Cd-doped and PbTe-alloyed PbSe. (b) Room-temperature lattice parameter of Pb0.98Na0.02Se1−yTey as a function of y. Data from earlier reports on PbSe−PbTe ternary alloys[6,20,21] are also incorporated for comparison. The solid line is a guide to the eye. (c) High-resolution TEM image of y = 0.15 sample showing clean matrix. Inset: diffraction pattern along (111) direction reveals that the crystal structure matches rock-salt structure (space group: Fm3m). (d) Lower-magnification TEM image for y = 0.15 sample and corresponding energy-dispersive mappings.

2. RESULTS AND DISCUSSION

2.1. Accelerating Band Convergence and Lowering Thermal Conductivity of p-type PbSe.

The powder X-ray diffraction (XRD) patterns of spark plasma sintering (SPS) processed $Pb_{0.98}Na_{0.02}Se_{1-y}Te_y$ (y = 0−0.2) samples can be indexed to the rock-salt structure with no second phase being observed within the instrument detection limits (Figure S1). The lattice parameters of $Pb_{0.98}Na_{0.02}Se_{1-y}Te_y$ (y = 0−0.2) together with those of other PbSe−PbTe alloys from the literature[6,20,21] as a function of y follow a simple Vegard's law (Figure 1b). In addition, the transmission electron microscopy (TEM) images for y = 0 and y = 0.15 samples show a clean matrix with no precipitates present (Figures S2 and 1c). Energy-dispersive spectroscopy (EDS) mappings suggest that all elements are distributed homogeneously in the y = 0.15 sample (Figure 1d). These results suggest that PbSe and PbTe form continuous solid solutions within the full composition range, which is consistent with previous studies.[6,22] Figure S3 shows the thermoelectric transport properties of $Pb_{0.98}Na_{0.02}Se_{1-y}Te_y$ (y = 0−0.2) as a function of temperature. σ decreases gradually with increasing y, probably due to the negative influence of PbTe alloying on the charge carrier mobility (μ) (Figure S3a). On the other hand, the Seebeck coefficient of $Pb_{0.98}Na_{0.02}Se$ is enhanced by introducing Te at Se lattice sites, especially at elevated temperatures (T > 500 K) (Figure S3b).

For materials[7,17,23−25] featuring two valence bands (inset of Figure 2a), which tend to converge with rising temperature, there is a redistribution of charge carriers between the two bands, leading to temperature-dependent Hall coefficient (RH) and a maximum (Figure 2a). RH peaks when the two bands contribute equally to charge transport.11,26,27 Therefore, RH peak temperature (TH) is an important measure of ΔEV. In other words, the lower TH is, the smaller ΔEV would be. We note that y = 0.15 has a lower TH (∼600 K) than y = 0 sample (∼700 K). This suggests that PbTe alloying makes band convergence occur earlier in PbSe.

We further employ the two-band Kane model28,29 to simulate the temperature dependence of carrier concentration (p) and S for y = 0 and y = 0.15 samples. A mobility ratio b = 4 and a temperature-dependent band gap $E_g = 0.17 + (3 \times 10^{-4})\ T$ (in K) are considered for PbSe.11 Other parameters, including the nonparabolicity parameter β (1.75 for LVB, 0 for HVB) and constant density-of-states effective masses m_d^* (0.27 m_e for LVB and 2.5 m_e for HVB; m_e is the rest electron mass),30 are also used in this model. With these, the temperature-dependent ΔEV can be extracted; see Figure 2b. For comparison, we also include ΔEV data of PbSe and PbTe measured by diffuse reflectance infrared Fourier transform spectroscopy (DRIFTS);31 see the dotted lines in Figure 2b. It is seen that the ΔEV values of PbSe simulated by two-band Kane model and obtained from DRIFTS measurement agree with each other quite well over the entire temperature range, validating the reliability of our fittings. Moreover, ΔEV decreases faster with heating in PbTe than in PbSe, which is in good agreement with previous studies.[11,13,17]

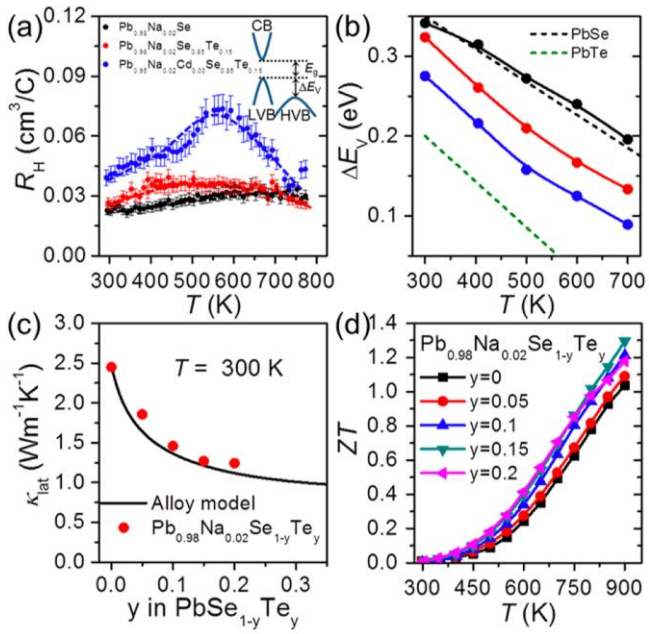

Figure 2. Temperature-dependent (a) Hall coefficients and (b) ΔE_V for Pb0.98Na0.02Se, Pb0.98Na0.02Se0.85Te0.15, and Pb0.95Na0.02Cd0.03Se0.85Te0.15. The ΔE_V data[31] (dotted lines) on pure PbSe and PbTe determined by DRIFTS are also included for comparison. (c) Room-temperature lattice thermal conductivity of Pb0.98Na0.02Se1−yTey as a function of y. The dotted lines shown in (a) are guides to the eye. Inset of (a) schematically shows the electronic band structure of PbSe: the band gap (E_g) separates the conduction band (CB) from the light valence band (LVB); another heavy valence band (HVB), also contributing to transport, is lower than LVB in energy by a magnitude of ΔE_V. The solid line in (c) is calculated by an alloying scattering model.[32,33] (d) ZT values as a function of temperature for Pb0.98Na0.02Se1−yTey.

Our simulations also show that the values of ΔEV at 300 K are quite similar for y = 0 and y = 0.15 samples, which is reasonable considering the small VBM energy difference of 0.21 eV between PbSe and PbTe (see Figure 5b). However, with rising temperature, accelerated by PbTe alloying, ΔE_V in PbSe0.85Te0.15 decreases much faster than that in the Te-free sample, shifting the band convergence to occur earlier in PbSe (Figure 2a). This is also supported by our first-principles electronic band structure calculations shown in Figure S4, which show very similar ΔE_V for PbSe (0.28 eV) and Pb27Se25Te2 (0.25 eV) at 0 K. However, this value becomes twice larger at 800 K (ΔE_V = 0.24 eV for PbSe and 0.18 eV for Pb27Se25Te2).

The thermal conductivity values are significantly lowered as PbTe is alloyed into PbSe, because both κ_{car} and κ_{lat} are lowered (Figure S3c and d). The details of calculating κ_{car} and κ_{lat} can be found in the Supporting Information, and the temperature-dependent thermal diffusivities (D), Lorentz numbers (L), and κ_{car} for all samples in this study are plotted in Figure S5. The Debye−Callaway model[32,33] has been successfully employed to quantitatively predict the κ_{lat} of lead and tin chalcogenides alloys.[24,34] In this model, mass and size contrasts between host and guest atoms are considered to cause scattering of phonons in a solid solution. We use this model to predict κlat of Pb0.98Na0.02Se1−xTex alloys, with the following input parameters: Debye temperature ΘD = 191 K,[9] average speed velocity υ = 1960 m/s,[9] and lattice inharmonic

constant ε = 110.34 The simulation results are shown as a solid curve in Figure 2c. We can see that the experimental values of κlat in this study agree well with the predicted ones. This again confirms the solid solution behavior between PbSe and PbTe and suggests that alloy scattering should account for the reduction of κlat in our Pb0.98Na0.02Se1−xTex alloys. Because of the great enhancement of S (Figure S3b) and notable reduction of κlat (Figure S3c) in PbSe by alloying with PbTe, a peak ZT of 1.3 at ∼900 K is reached for the sample with y = 0.15, which is 30% improvement over the Te-free sample (Figure 2d). Below we proceed to optimize the thermoelectric performance of PbSe0.85Te0.15 by doping 3 mol % Cd at Pb lattice sites and by adjusting the Na doping concentration.

2.2. Enhancing Band Convergence in Cd-substituted PbSe0.85Te0.15 Alloys and Band Alignment. Powder XRD pattern suggest that SPS-processed Pb0.97−xNaxCd0.03Se0.85Te0.15 (x = 0.005−0.025) samples show single-phase rock-salt PbSe structure (Figure S6). However, the TEM image of x = 0.02 sample unambiguously shows the presence of 30−80 nm precipitates, mostly along grain boundaries (Figure 3a). EDS elemental mappings suggest that these precipitates are rich in Cd and poor in Pb, while other elements (Na, Se, and Te) are homogeneously distributed nearly everywhere (Figure 3b−g). Therefore, it can be concluded that at the 3 mol % level Cd does not fully enter into the lattice sites of PbSe and partly precipitates as second phase, the chemical composition of which can be approximately designated as CdSe1−yTey. This is similar to what was found in Pb0.98Na0.02Se-3%CdSe where CdSe nanoscale precipitates are present.[18] The temperature-dependent thermoelectric transport properties of Pb0.97−xNaxCd0.03Se0.85Te0.15 (x = 0.005−0.025) are shown in Figure 4. σ first increases with increasing x, reaches the highest value at x = 0.02, and then decreases (Figure 4a). Figure 5a plots the room-temperature mobility μ as a function of p for p-type Na-doped PbSe, Pb0.97Cd0.03Se, and Pb0.97Cd0.03Se0.85Te0.15. For all samples, log μ linearly decreases with increasing log p. It is reasonable that the hole mobilities will be lower in Pb0.97Cd0.03Se than in pure PbSe because of poor band alignment of CdSe precipitates, as discussed in our previous report.[18] Surprisingly, when 15% of Se atoms are replaced by Te atoms resulting in a composition of Pb0.97Cd0.03Se0.85Te0.15, we find that the holes have larger mobility than in Pb0.97Cd0.03Se. For example, at p = ∼3 × 1020 cm−3, the hole mobilities of Pb0.97Cd0.03Se0.85Te0.15 and Pb0.97Cd0.03Se are ∼32 and ∼21 cm2 V−1 s−1, respectively.

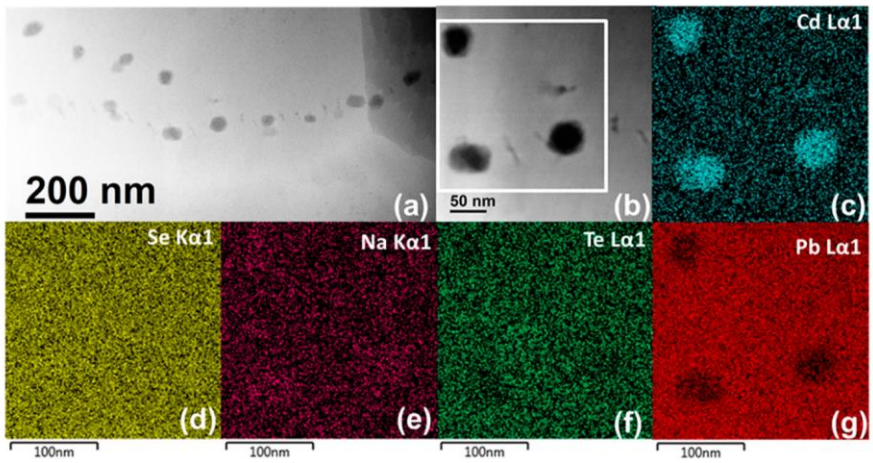

Figure 3. (a) TEM image of the sample Pb0.95Na0.02Cd0.03Se0.85Te0.15. (b) Zoomed-in view of (a) and the corresponding elemental distribution mappings: (c) Cd, (d) Se, (e) Na, (f) Te, and (g) Pb.

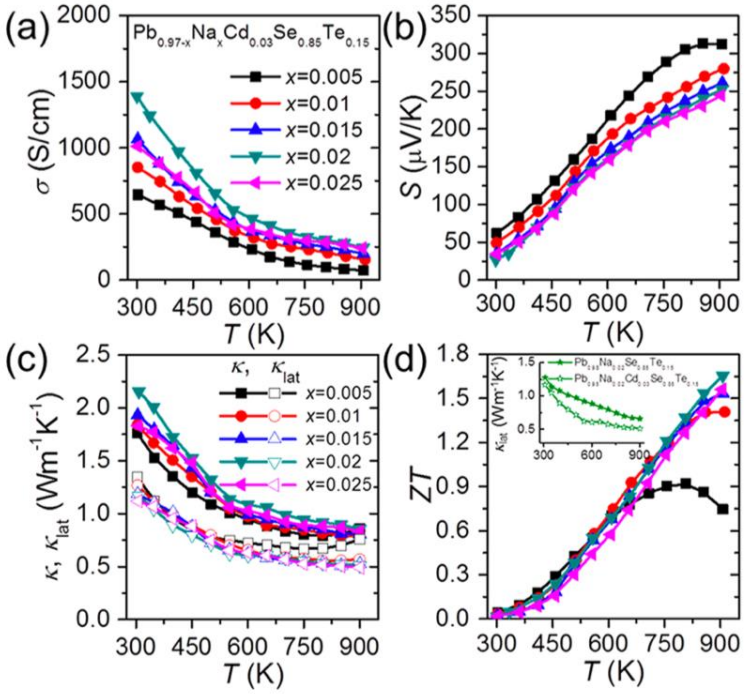

Figure 4. Thermoelectric transport properties of Pb0.97−xNaxCd0.03Se0.85Te0.15 (x = 0.005−0.025) as a function of temperature: (a) electrical conductivity, (b) Seebeck coefficient, (c) (lattice) thermal conductivity, and (d) ZT values. Inset of (d) is a comparison of temperature-dependent κ_{lat} between 2 mol % Na-doped PbSe0.85Te0.15 and Pb0.97Cd0.03Se0.85Te0.15.

To better understand the high mobility in Pb0.97Cd0.03Se0.85Te0.15, we experimentally determined the VBM energies of Pb0.98Na0.02Se, Pb0.98Na0.02Te, and

Pb0.98Na0.02Se0.85Te0.15 by photoemission yield spectroscopy measurements (Table S1). In combination with the experimental data reported for CdSe and CdTe,[35] we are able to plot the VBM energy diagram of these compounds in Figure 5b. It is seen that the VBM of CdSe lies ~0.32 eV below that of PbSe, which agrees with an earlier study[18] and indicates a nonoptimal valence band alignment. This value is large enough to impede charge flow across the PbSe/CdSe interfaces (Figure 5c). As we alloy PbSe matrix with PbTe, we can see that the VBM energy of PbSe0.85Te0.15 is slightly elevated by only 0.06 eV in comparison to PbSe (the VBM of PbTe is ~0.21 eV higher than that of PbSe). However, because the VBM of CdTe is ~0.49 eV above that of CdSe,35 CdSe1−yTey has a much higher VBM energy than CdSe based on the solid solution principle. As a result, the valence band energy offsets between PbSe0.85Te0.15 and CdSe1−yTey are significantly reduced compared to the case between PbSe and CdSe, resulting in a good band alignment. As a result, high μ is maintained in this system (Figure 5d). This is quite similar to what has been demonstrated in the PbTe−SrTe system.[4,5]

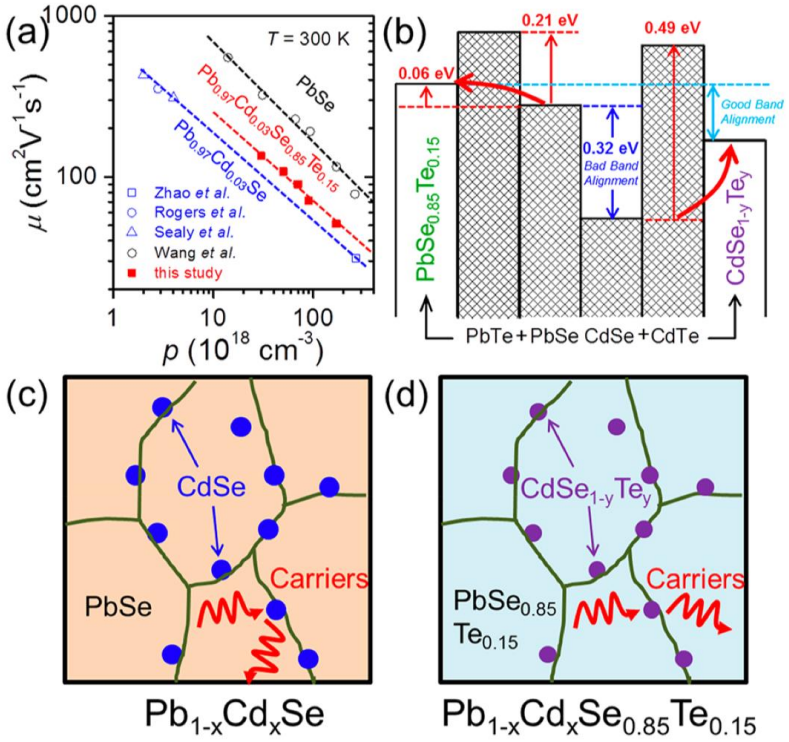

Figure 5. (a) Room-temperature carrier mobilities μ as a function of carrier concentration p for p-type doped PbSe, Pb0.97Cd0.03Se, and Pb0.97Cd0.03Se0.85Te0.15. (b) VBM energy diagram of Pb0.98Na0.02Te and Pb0.98Na0.02Se0.85Te0.15 relative to that of PbSe measured by photoemission yield spectroscopy. The data of CdSe and CdTe obtained using the same method35 are also included for comparison. Schematic phase mappings in the samples (c) Pb0.97Cd0.03Se and (d) Pb0.97Cd0.03Se0.85Te0.15. In (c), the VBM energy between the matrix (PbSe) and the precipitate is large (~0.32 eV), resulting in strong scattering of charge carriers at the matrix/precipitate interfaces. In (d), VBM energy difference is significantly reduced between the matrix (PbSe0.85Te0.15) and the precipitate (CdSe1−yTey) by incorporating Te, so that charge carriers are less scattered at these interfaces.

Despite the much improved σ by increasing Na concentration, the S and κ of Pb0.97−xNaxCd0.03Se0.85Te0.15 (x = 0.005−0.025) are only moderately decreased and increased, respectively, in this process (Figure 4b and c). It has been demonstrated that Cd substituting Pb in PbSe converges the LVB and HVB by enlarging the band gap.18 Indeed, our infrared spectroscopy measurements (Figure 5a) suggest that, while 15% PbTe alloying hardly changes the optical band gap of PbSe, the introduction of 3 mol % of Cd replacing Pb leads to ∼40% increase of Eg (from ∼0.23 to ∼0.32 eV) at room temperature.

We calculated ΔEV as a function of temperature for Pb0.97−xNaxCd0.03Se0.85Te0.15 by fitting the temperature-dependent values of S and RH (high-temperature RH is shown in Figure 2a) as described earlier (Figure 2b). We can see that ΔEV of Pb0.95Na0.02Cd0.03Se0.85Te0.15 is reduced at all temperatures in comparison with that of Pb0.98Na0.02Se0.85Te0.15, and the two samples have almost the same temperature dependence of ΔEV. This further demonstrates the valence band convergence effect in PbSe by Cd substitution and also suggests that valence band convergence acceleration effect by PbTe alloying still works well even if Cd is incorporated. Because of the synergistic effects of PbTe alloying and Cd substitution on the electronic bands, ΔE V of Pb0.95Na0.02Cd0.03Se0.85Te0.15 is reduced to as low as ∼0.1 eV at 700 K, within 2kBT of one another at this temperature. This demonstrates that the new modified electronic structure enables the valence band convergence in PbSe to occur at sufficiently low temperatures. For comparison, the valence band convergence temperature in pure PbSe is believed to occur fully at 1000 K, according to results based on optical absorption spectra.31 Another important proof of improved band degeneracy in Pb1−xCdxSe1−yTey is that its Hall peak temperature (∼550 K) is significantly lower than that of PbSe (∼700 K); see Figure 2a.

The temperature-dependent Seebeck coefficients of Nadoped PbSe, PbSe0.85Te0.15, and Pb0.97Cd0.03Se0.85Te0.15 are compared at the same p of $\sim 2 \times 10^{20}$ cm−3 (Figure 6b). It can be seen that PbSe and PbSe0.85Te0.15 have very similar values of S around room temperature, consistent with the similar ΔE_V. However, the S of PbSe0.85Te0.15 increases more rapidly with temperature and is significantly higher at elevated temperatures than that of PbSe. This difference in temperature dependence of S between the two samples is in good agreement with our band convergence acceleration model in PbTe-alloyed PbSe. On the other hand, Pb0.97Cd0.03Se0.85Te0.15 has higher values of S than PbSe0.85Te0.15 in the entire temperature range, and the two samples roughly have the same S dependence on T. This further verifies the valence band convergence effect by Cd substitution in PbSe and is also consistent with the fact that band convergence acceleration effect by PbTe alloying is preserved after Cd is added.

As shown in Figure 4c, κ_{lat} is slightly reduced with increasing Na content around room temperature because of enhanced point defect scattering of Na dopants against heat-carrying phonons. At high temperatures (T > 500 K), samples with high Na concentrations ($x \geqslant 0.01$) have much lower κ_{lat} in comparison to the one with x = 0.005. We attribute this to the suppression of bipolar diffusion[36] in the heavily doped samples. The inset of Figure 4d shows a comparison of temperature dependent κ_{lat} between 2 mol % Na-doped Pb0.97Cd0.03Se0.85Te0.15 and PbSe0.85Te0.15. It is seen that κlat of PbSe0.85Te0.15 is reduced by 3 mol % Cd substitution for Pb because Cd replacing Pb creates more lattice point defects and any excess Cd precipitates out as CdSe1−yTey (Figure 3), with both events

generating strong phonon scattering. The lowest κlat is ∼0.5 W m−1 K−1 at T > 700 K in the samples with x ⩾ 0.01, which already approaches the theoretical minimum thermal conductivity of ∼0.38 W m−1 K−1 for PbSe estimated by the modified Cahill model.37 We attribute this to the formation of all-scale hierarchical microstructures (point defects, nanostructures, and mesoscale grain boundaries)4,7 in our samples.

The maximum ZT of 1.7 at ∼900 K is obtained in the Pb0.95Na0.02Cd0.03Se0.85Te0.15 sample, which is ∼70% higher than the control sample of Pb0.98Na0.02Se and among the highest values reported for a PbSe-based system; see Figures 4d and 6c. Our sample outperforms not only in peak ZT (1.7 at ∼900 K) but more importantly in average ZT (∼1 between 400 and 900 K) as well (Figure 6d). This top thermoelectric performance enables PbSe to be a very competitive substitute of PbTe.

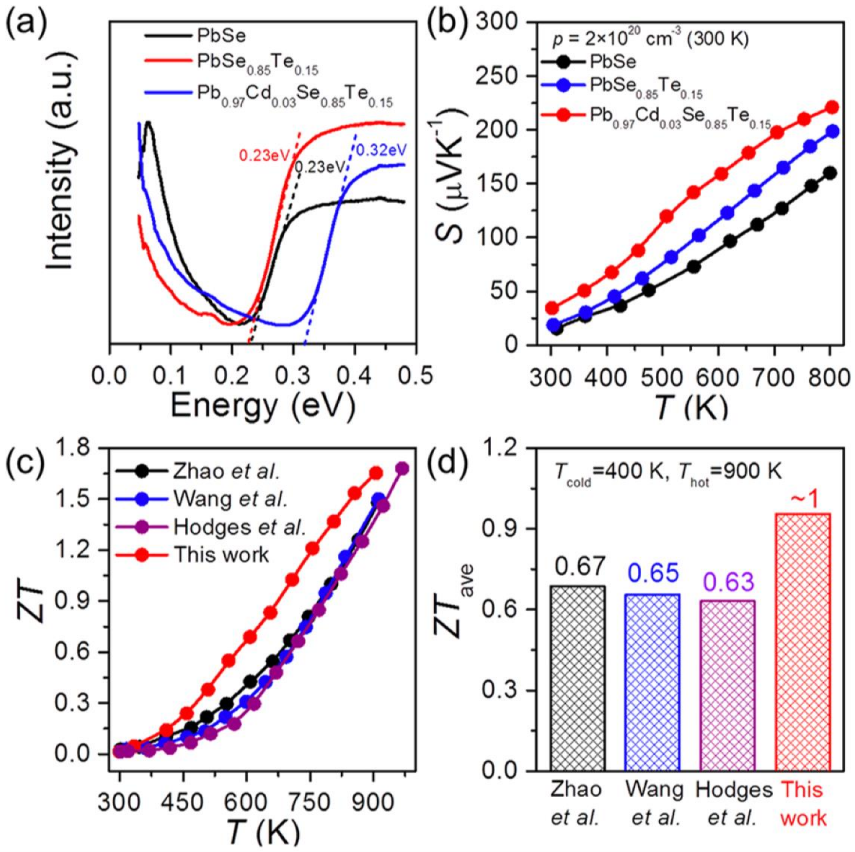

Figure 6. (a) Room-temperature infrared spectrum for undoped PbSe, Pb0.97Cd0.03Se, and Pb0.97Cd0.03Se0.85Te0.15. (b) Comparison of temperature-dependent S for p-type doped PbSe,17 Pb0.97Cd0.03Se,18 and Pb0.97Cd0.03Se0.85Te0.15 with the same p of ∼2 × 1020 cm−3 (roomtemperature value). Comparisons of (c) temperature-dependent ZT values and (d) 400−900 K ZT_{ave} between this work and previous reports17−19 on best performing p-type PbSe thermoelectric materials.

3. CONCLUDING REMARKS

PbTe alloying in PbSe plays several key roles in enhancing the thermoelectric performance of PbSe: (i) it accelerates valence band convergence because ΔE_V decreases more rapidly with rising temperature in PbTe than in PbSe; (ii) it lowers the VBM energy difference between matrix and precipitate, thereby facilitating valence band alignment for improved charge carrier mobility; (iii) it reduces κ_{lat} by alloying effect in addition to Cd doping and Cd-containing nanostructures. Furthermore, Cd substitution for PbSe0.85Te0.15 further converges LVB and HVB by enlarging the band gap, leading to enhanced band degeneracy for higher Seebeck coefficients. We have thus reached a peak ZT of ~1.7 at 900 K and a record high ZT_{ave} of ~1 at TC = 400 K and TH = 900 K in p-type Pb0.95Cd0.03Se0.85Te0.15. It yields a theoretical conversion efficiency,

$$\eta = \frac{T_H - T_C}{T_H} \frac{(1 + ZT_{ave})^{1/2} - 1}{(1 + ZT_{ave})^{1/2} + \frac{T_C}{T_H}}$$

of ~12.4%. This work goes beyond conventional band convergence and highlights a rational design of favorable convergence of electronic bands for achieving high thermoelectric performance in a variety of materials.

ACKNOWLEDGMENTS

G.T. acknowledges the financial support from the Natural Science Foundation of China (Grant no. 11804261). At Northwestern University the work was supported primarily by the Department of Energy, Office of Science, Basic Energy Sciences under Grant DE-SC0014520 (synthesis, sample processing, transport, and TEM and DFT calculations). Photoemission yield spectroscopy measurements were carried out with equipment acquired by ONR Grant N00014-18-12102. Transmission electron microscopy work was partially performed in the EPIC facility of the NUANCE Center at Northwestern University. Access to facilities of high-performance computational resources at Northwestern University is acknowledged.

REFERENCES

(1) Tan, G.; Zhao, L.-D.; Kanatzidis, M. G. Rationally Designing High-Performance Bulk Thermoelectric Materials. Chem. Rev. 2016, 116 (19), 12123−12149.

(2) Bell, L. E. Cooling, Heating, Generating Power, and Recovering Waste Heat with Thermoelectric Systems. Science 2008, 321 (5895), 1457−1461.

(3) Hsu, K. F.; Loo, S.; Guo, F.; Chen, W.; Dyck, J. S.; Uher, C.; Hogan, T.; Polychroniadis, E. K.; Kanatzidis, M. G. Cubic
AgPbmSbTe2+mBulk Thermoelectric Materials with High Figure of Merit. Science 2004, 303 (5659), 818−821.

(4) Biswas, K.; He, J.; Zhang, Q.; Wang, G.; Uher, C.; Dravid, V. P.; Kanatzidis, M. G. Strained endotaxial nanostructures with high thermoelectric figure of merit. Nat. Chem. 2011, 3, 160.

(5) Biswas, K.; He, J.; Blum, I. D.; Wu, C.-I.; Hogan, T. P.; Seidman, D. N.; Dravid, V. P.; Kanatzidis, M. G. High-performance bulk thermoelectrics with all-scale hierarchical architectures. Nature 2012, 489, 414.
(6) Pei, Y.; Shi, X.; LaLonde, A.; Wang, H.; Chen, L.; Snyder, G. J. Convergence of electronic bands for high performance bulk thermoelectrics. Nature 2011, 473, 66.
(7) Tan, G.; Shi, F.; Hao, S.; Zhao, L.-D.; Chi, H.; Zhang, X.; Uher, C.; Wolverton, C.; Dravid, V. P.; Kanatzidis, M. G. Non-equilibrium processing leads to record high thermoelectric figure of merit in PbTe−SrTe. Nat. Commun. 2016, 7, 12167.
(8) Heremans, J. P.; Jovovic, V.; Toberer, E. S.; Saramat, A.; Kurosaki, K.; Charoenphakdee, A.; Yamanaka, S.; Snyder, G. J. Enhancement of Thermoelectric Efficiency in PbTe by Distortion of the Electronic Density of States. Science 2008, 321 (5888), 554−557. (9) Wang, H.; Pei, Y.; LaLonde, A. D.; Snyder, G. J. Heavily Doped p-Type PbSe with High Thermoelectric Performance: An Alternative for PbTe. Adv. Mater. 2011, 23 (11), 1366−1370.
(10) Wang, H.; Pei, Y.; LaLonde, A. D.; Snyder, G. J. Weak electron−phonon coupling contributing to high thermoelectric performance in n-type PbSe. Proc. Natl. Acad. Sci. U. S. A. 2012, 109 (25), 9705−9709.
(11) Ravich, I. I.; Efimova, B. A.; Smirnov, I. A. Semiconducting lead chalcogenides; Plenum Press: New York, 1970; Vol. 5.
(12) Sitter, H.; Lischka, K.; Heinrich, H. Structure of the second valence band in PbTe. Phys. Rev. B 1977, 16 (2), 680−687.
(13) Tauber, R. N.; Machonis, A. A.; Cadoff, I. B. Thermal and Optical Energy Gaps in PbTe. J. Appl. Phys. 1966, 37 (13), 4855− 4860.
(14) Pei, Y.; Wang, H.; Gibbs, Z. M.; LaLonde, A. D.; Snyder, G. J. Thermopower enhancement in Pb1−xMnxTe alloys and its effect on thermoelectric efficiency. NPG Asia Mater. 2012, 4, No. e28.
(15) Pei, Y.; LaLonde, A. D.; Heinz, N. A.; Snyder, G. J. High Thermoelectric Figure of Merit in PbTe Alloys Demonstrated in PbTe−CdTe. Adv. Energy Mater. 2012, 2 (6), 670−675.
(16) Zhao, L. D.; Wu, H. J.; Hao, S. Q.; Wu, C. I.; Zhou, X. Y.; Biswas, K.; He, J. Q.; Hogan, T. P.; Uher, C.; Wolverton, C.; Dravid, V. P.; Kanatzidis, M. G. All-scale hierarchical thermoelectrics: MgTe in PbTe facilitates valence band convergence and suppresses bipolar thermal transport for high performance. Energy Environ. Sci. 2013, 6 (11), 3346−3355.
(17) Wang, H.; Gibbs, Z. M.; Takagiwa, Y.; Snyder, G. J. Tuning bands of PbSe for better thermoelectric efficiency. Energy Environ. Sci. 2014, 7 (2), 804−811.
(18) Zhao, L.-D.; Hao, S.; Lo, S.-H.; Wu, C.-I.; Zhou, X.; Lee, Y.; Li, H.; Biswas, K.; Hogan, T. P.; Uher, C.; Wolverton, C.; Dravid, V. P.; Kanatzidis, M. G. High Thermoelectric Performance via Hierarchical Compositionally Alloyed Nanostructures. J. Am. Chem. Soc. 2013, 135 (19), 7364−7370.
(19) Hodges, J. M.; Hao, S.; Grovogui, J. A.; Zhang, X.; Bailey, T. P.; Li, X.; Gan, Z.; Hu, Y.-Y.; Uher, C.; Dravid, V. P.; Wolverton, C.; Kanatzidis, M. G. Chemical Insights into PbSe−x%HgSe: High Power Factor and Improved Thermoelectric Performance by Alloying with Discordant Atoms. J. Am. Chem. Soc. 2018, 140 (51), 18115−18123. (20) Poudeu, P. F. P.; D'Angelo, J.; Kong, H.; Downey, A.; Short, J. L.; Pcionek, R.; Hogan, T. P.; Uher, C.; Kanatzidis, M. G. Nanostructures versus Solid Solutions: Low Lattice Thermal Conductivity and Enhanced

Thermoelectric Figure of Merit in Pb9.6Sb0.2Te10-xSex Bulk Materials. J. Am. Chem. Soc. 2006, 128 (44), 14347−14355.
(21) Li, J. Q.; Li, S. P.; Wang, Q. B.; Wang, L.; Liu, F. S.; Ao, W. Q. Synthesis and thermoelectric properties of the PbSe1−xTex alloys. J. Alloys Compd. 2011, 509 (13), 4516−4519.
(22) Wang, H.; LaLonde, A. D.; Pei, Y.; Snyder, G. J. The Criteria for Beneficial Disorder in Thermoelectric Solid Solutions. Adv. Funct. Mater. 2013, 23 (12), 1586−1596.
(23) Wu, D.; Zhao, L.-D.; Hao, S.; Jiang, Q.; Zheng, F.; Doak, J. W.;
Wu, H.; Chi, H.; Gelbstein, Y.; Uher, C.; Wolverton, C.; Kanatzidis, M.; He, J. Origin of the High Performance in GeTe-Based Thermoelectric Materials upon Bi2Te3 Doping. J. Am. Chem. Soc. 2014, 136 (32), 11412−11419.
(24) Tan, G.; Shi, F.; Hao, S.; Chi, H.; Bailey, T. P.; Zhao, L.-D.; Uher, C.; Wolverton, C.; Dravid, V. P.; Kanatzidis, M. G. Valence Band Modification and High Thermoelectric Performance in SnTe Heavily Alloyed with MnTe. J. Am. Chem. Soc. 2015, 137 (35), 11507−11516.
(25) Tan, G.; Shi, F.; Doak, J. W.; Sun, H.; Zhao, L.-D.; Wang, P.; Uher, C.; Wolverton, C.; Dravid, V. P.; Kanatzidis, M. G. Extraordinary role of Hg in enhancing the thermoelectric performance of p-type SnTe. Energy Environ. Sci. 2015, 8 (1), 267−277.
(26) Tan, G.; Zhao, L.-D.; Shi, F.; Doak, J. W.; Lo, S.-H.; Sun, H.; Wolverton, C.; Dravid, V. P.; Uher, C.; Kanatzidis, M. G. High Thermoelectric Performance of p-Type SnTe via a Synergistic Band Engineering and Nanostructuring Approach. J. Am. Chem. Soc. 2014, 136 (19), 7006−7017.
(27) Tan, G.; Shi, F.; Hao, S.; Chi, H.; Zhao, L.-D.; Uher, C.; Wolverton, C.; Dravid, V. P.; Kanatzidis, M. G. Codoping in SnTe: Enhancement of Thermoelectric Performance through Synergy of Resonance Levels and Band Convergence. J. Am. Chem. Soc. 2015, 137 (15), 5100−5112.
(28) Kane, E. O. Semiconductors and semimetals; Academic Press: New York, 1972; Vol. 9.
(29) Chi, H.; Tan, G.; Kanatzidis, M. G.; Li, Q.; Uher, C. A lowtemperature study of manganese-induced ferromagnetism and valence band convergence in tin telluride. Appl. Phys. Lett. 2016, 108 (18), 182101.
(30) Chasapis, T. C.; Lee, Y.; Hatzikraniotis, E.; Paraskevopoulos, K. M.; Chi, H.; Uher, C.; Kanatzidis, M. G. Understanding the role and interplay of heavy-hole and light-hole valence bands in the thermoelectric properties of PbSe. Phys. Rev. B: Condens. Matter Mater. Phys. 2015, 91 (8), 085207.
(31) Gibbs, Z. M.; Kim, H.; Wang, H.; White, R. L.; Drymiotis, F.; Kaviany, M.; Snyder, G. J. Temperature dependent band gap in PbX (X = S, Se, Te). Appl. Phys. Lett. 2013, 103 (26), 262109.
(32) Callaway, J. Model for Lattice Thermal Conductivity at Low Temperatures. Phys. Rev. 1959, 113 (4), 1046−1051.
(33) Callaway, J.; von Baeyer, H. C. Effect of Point Imperfections on Lattice Thermal Conductivity. Phys. Rev. 1960, 120 (4), 1149−1154.
(34) Wang, H.; Wang, J.; Cao, X.; Snyder, G. J. Thermoelectric alloys between PbSe and PbS with effective thermal conductivity reduction and high figure of merit. J. Mater. Chem. A 2014, 2 (9), 3169−3174.
(35) Jasieniak, J.; Califano, M.; Watkins, S. E. Size-Dependent Valence and Conduction Band-Edge Energies of Semiconductor Nanocrystals. ACS Nano 2011, 5 (7), 5888−5902.

(36) Drabble, J. R.; Goldsmid, H. J. Thermal conduction in semiconductors; Pergamon: 1961; Vol. 4.
(37) Cahill, D. G.; Watson, S. K.; Pohl, R. O. Lower limit to the thermal conductivity of disordered crystals. Phys. Rev. B: Condens. Matter Mater. Phys. 1992, 46 (10), 6131−6140.